Published in final edited form as:
IEEE Trans Biomed Eng. 2013 October ; 60(10): 2858–2866. doi:10.1109/TBME.2013.2264162.

Point Process Modeling of Interbreath Interval: A New Approach for the Assessment of Instability of Breathing in Neonates

Premananda Indic [Member, IEEE],
Department of Neurology, University of Massachusetts Medical School, MA 01655 USA

David Paydarfar, and
Department of Neurology, University of Massachusetts Medical School, MA 01655, USA and also with Wyss Institute, Harvard University, Boston, MA 02115 USA

Riccardo Barbieri [Senior Member, IEEE]
Department of Anesthesia, Critical Care, and Pain Medicine, Massachusetts General Hospital, Harvard Medical School, Boston, MA 02114 USA, and also with the Department of Brain and Cognitive Sciences, Massachusetts Institute of Technology, Cambridge, MA 02139 USA

Premananda Indic: Premananda.Indic@umassmed.edu; David Paydarfar: David.Paydarfar@umassmed.edu; Riccardo Barbieri: barbieri@neurostat.mit.edu

Abstract

Interbreath interval (IBI), the time interval between breaths, is an important measure used to analyze irregular breathing patterns in neonates. The discrete bursts of neural activity generate the IBI time series, which exhibits stochastic as well as deterministic dynamics. To quantify the irregularity of breathing, we propose a point process model of IBI using a comprehensive stochastic dynamic modeling framework. The IBIs of immature breathing patterns exhibit a long tail distribution and within a point process model, we have considered the lognormal distribution to represent the stochastic IBI characteristics. An autoregressive (AR) function is embedded within the model to capture the short-term IBI dynamics including abrupt IBI prolongations related to sporadic and periodic apneas that are common in neonates. We tested the utility of our paradigm for depicting the respiratory dynamics in neonatal rats and in preterm infants. Kolmogorov–Smirnov (KS) and independence tests reveal that the model accurately tracks the dynamic characteristics of the signals. In preterm infants, our model-derived indices of IBI instability strongly correlate with clinically derived indices of maturation. Our results validate a new class of algorithms, based on the point process theory, for defining instantaneous measures of breathing irregularity in neonates.

Index Terms

Infant apnea; lognormal distribution; point processes; prematurity; respiratory rhythm; time-frequency analysis

Correspondence to: Premananda Indic, Premananda.Indic@umassmed.edu.

Color versions of one or more of the figures in this paper are available online at http://ieeexplore.ieee.org.

I. Introduction

Respiratory rhythm in mammals is governed by neural circuits within the brainstem that signal the timing and depth of each breath [1]. Respiratory neurons exhibit the recurrent bursts of action potentials that drive phrenic and other respiratory motor neurons to produce continuous ventilation. The immaturity of the brainstem circuits governing respiratory rhythm can result in irregular breathing patterns with prolonged apneic pauses, a common clinical problem in infants with postconceptional age less than 36 weeks. The apnea of prematurity is a common cause of recurrent episodes of severe hypoxemia that has been associated with acute multiorgan dysfunction, developmental delay, and subsequent cognitive impairments [2], [3].

The interval between successive inspirations, the interbreath interval (IBI), is an important measure of breathing patterns in neonates. However, breathing patterns are highly nonstationary, with rapid changes in measures of breathing and to date there is no algorithm available that can capture instantaneous changes of IBI. The previous analyses of IBI in infants reveals stochastic characteristics with a long-tail distribution [4] as well as deterministic dynamic characteristics, for example low frequency oscillations with periodic apneas [5]. Hence, we propose to develop an algorithm that can capture both the stochastic as well as deterministic dynamic characteristics of IBI, providing a framework for computing the instantaneous estimates of variability in breathing.

A basic assumption of our model is that the peak of inspiration, marked by the peak of inhalation recorded noninvasively, represents a discrete event that marks the timing of neuronal inspiratory bursts. A second assumption is that IBI dynamics are governed by continuous processes under the regulation of multiple feed-back and feed-forward loops impinging upon the brainstem respiratory oscillator. Our model should be able to track the instability of breathing in real time and could provide the risk stratification of the respiratory system that might help clinicians to devise appropriate interventions for treatment of apnea of prematurity [3], [6], [7].

Within a point process model, we considered the lognormal distribution to represent the stochastic nature of IBI and include a higher p-order autoregressive (AR(p)) model to describe the dynamic nature of the IBI. The choice of the lognormal distribution was inspired by previous work done on infants, in which it was shown that IBI in infants follows a long-tail distributionwith the characterizing parameter that changes with maturation [4].

The AR(p) model, a reliable and a simplistic representation, is considered as a starting point to represent the IBI dynamics. We estimated the time varying parameters of the point process model by maximum local likelihood approach and assess the model goodness-of-fit by a Kolmogorov–Smirnov (KS) test derived from a time rescaling theorem [8]. We illustrate our approach using data from newborn rat as well as preterm infant recordings, both exhibiting irregular breathing patterns with apnea. A preliminary version of this study has been reported in [9].

II. Methods

In this section, we present the point process modeling framework that integrates the stochastic model of IBI along with the dynamic state-space model of IBI, the local likelihood approach for deriving the instantaneous estimate of the model and the goodness-of-fit tests to evaluate the performance of the model. Our model provides a precise probabilistic description of the IBI at any desired time resolution and allows estimating the dynamic variation of the parameters.

A. Stochastic Dynamic Model of IBI

Frey *et al*. [4] showed that IBI follows a power law distribution with its alpha exponent ranging from ~2.2 to ~3.7. There was a positive correlation between alpha exponent and maturational age, reflecting a reduction in the incidence of apnea/hypopnea that make up the long-tail distribution. We note that a power law distribution with an exponent less than 3 has infinite variance [4].

It has also been shown that for preterm infants, IBI variance correlates with the incidence of apnea [7]. Therefore, a finite variance is an important factor in defining infant respiratory physiology.

The implementation of a power law distribution is feasible within the point process framework, but the instantaneous assessment of the alpha exponent would drop below and rise above the threshold for finite variance. Thus, an important requirement for our study was to use a statistical model of IBI that defines a finite variance over the range of expected infant breathing patterns, and also includes the long-tail distribution as a feature of prolonged apnea. To capture these statistical characteristics in IBI, we propose the lognormal distribution which is mathematically related to the power law distribution [10] and has been considered in previous work on infants [11].

The IBI is derived from the time interval between successive peaks of the respiratory signal. We considered in an observation interval $(0, T]$, successive peaks of the respiratory signal, $0 < u_1 < u_2 <, \ldots\ldots, < u_k <, \ldots\ldots, < u_K \leq T$. Then, we assume that at any given peak u_k, the waiting time until next peak of the respiratory signal obeys a history dependent lognormal probability density $f(t|H_k, \theta)$ as

$$f(t|H_k,\theta) = \left[\frac{1}{2\pi\sigma^2 (t-u_k)^2}\right]^{\frac{1}{2}} \times exp\left\{-\frac{1}{2}\frac{(ln(t-u_k)-\mu(H_k,\theta))^2}{\sigma^2}\right\} \quad (1)$$

where t is any time, $t > u_k$, H_k is the history of the IBI up to u_k represented as $H_k = \{u_k, w_k, w_{k-1}, \ldots., w_{k-p+1}\}$ with $w_k = u_k - u_{k-1}$ is the kth IBI, and θ is a vector of model parameters. The probability density in (1) defines the stochastic characteristics of IBI with $\mu(H_k, \theta)$ and σ as the characterizing parameters that represents the mean and the standard deviation of the distribution. It can be shown that for a sufficiently large σ, the logarithm of the density function in (1) will be approximately linear with respect to the logarithm of IBI, thus reflecting more closely a power law distribution [10].

The instantaneous mean is modeled using a *p*-order autoregressive process, AR(*p*) as

$$\mu\left(H_k,\theta\right)=\theta_o+\sum_{j=1}^{p}\theta_j\, w_{k-j+1}. \quad (2)$$

The characterizing parameters are estimated at each instant of time, using a local maximum-likelihood approach in which $\theta(t)$ and $\sigma(t)$ are evaluated using an optimization procedure. Thus, the time varying representation of the parameters are obtained as

$$\mu_{IBI}\left(t\right)=\mu\left(H_k,\theta\left(t\right)\right) \quad (3)$$

$$\sigma_{IBI}\left(t\right)=\sigma\left(t\right). \quad (4)$$

From the lognormal probability density represented in (1), we can also evaluate additional instantaneous descriptors

$$\begin{aligned} M\left(t\right) &= e^{\mu(t)+\sigma(t)^2/2} \\ V\left(t\right) &= \left(e^{\sigma\left(t\right)^2}-1\right)\, e^{2\mu(t)+\sigma\left(t\right)^2} \\ S\left(t\right) &= \left(e^{\sigma\left(t\right)^2}+2\right)\, \sqrt{e^{\sigma\left(t\right)^2}-1} \\ K\left(t\right) &= e^{4\sigma\left(t\right)^2}+2\, e^{3\sigma\left(t\right)^2}+3\, e^{2\sigma\left(t\right)^2}-6. \end{aligned} \quad (5)$$

The descriptors *M* (*t*), *V* (*t*), *S* (*t*), and *K* (*t*) represent the instantaneous estimates of mean, variance, skewness, and kurtosis, respectively, of the lognormal probability density which can be estimated for any time resolution, Δ*t*.

We can further define the indices of a respiratory rate by considering the inverse variable $r = (t - u_k)^{-1}$ along with its probability density $f(r|H_k, \theta)$ obtained as

$$\begin{aligned} f\left(r|H_k,\theta\right) &= \left|\frac{dr}{dt}\right|\, f\left(t|H_k,\theta\right)=\left[\frac{1}{2\pi\,\sigma^2\,r^2}\right]^{\frac{1}{2}} \\ &\quad \times exp\left\{-\frac{1}{2}\frac{\left(ln\left(t-u_k\right)+\mu\left(H_k,\theta\right)\right)^2}{\sigma^2}\right\}. \end{aligned} \quad (6)$$

From the lognormal formulation, we can obtain the mean M_r and variance V_r of the respiratory rate by just setting $\mu = -\mu$ in the equation for *M* and *V*, respectively

$$\begin{aligned} M_r\left(t\right) &= e^{-\mu\left(t\right)+\sigma\left(t\right)^2/2} \\ V_r\left(t\right) &= \left(e^{\sigma\left(t\right)^2}-1\right)\, e^{-2\mu\left(t\right)+\sigma\left(t\right)^2}. \end{aligned} \quad (7)$$

The AR representation allows us to estimate the spectrum as well as identify the poles of the dynamics, both of which can provide a more detailed characterization of the instability of breathing. Using (2), we estimated the instantaneous spectrum as

$$P(\omega, t) = \sigma^2(t) \left| \frac{1}{1 - \sum_{j=1}^{p} \theta_j(t) e^{-2\pi j f_s}} \right|^2 \quad (8)$$

where $f_s = 1/\Delta t$ is the sampling frequency in Hz at which the parameters are estimated and the poles as the roots of the equation $\theta_o + \sum_{j=1}^{p} \theta_j w_{k-j+1}$. We represent the power spectrum in a time–frequency plane using a precision obtained by dividing the frequency range of 0 to $f_s/2$ in 512 equal parts. Thus, 512 corresponds to a frequency of $f_s/2$.

In summary, the descriptors that we employed to study the instantaneous characteristics of IBI include: 1) mean IBI, *M;* 2) variance of IBI, *V;* 3) skewness of IBI, *S;* 4) kurtosis of IBI, *K;* 5) mean respiratory rate, M_r; 6) variance of respiratory rate, V_r; 7) spectrum, and 8) poles. All these estimated parameters and descriptors provide a new approach for the assessment of instability of breathing in neonates.

B. Local Maximum Likelihood Approach

To compute optimal estimates of θ and σ, we can define the local joint probability density of $u_{t-l:t}$, with l being the length of the local likelihood observation interval. If we observe n_t peaks within this interval as $u_1 < u_2 <, \ldots\ldots, < u_{n_t} \leq t$ and if θ as well as σ are time varying, then at time t, we estimate the maximum likelihood estimate of $\hat{\theta_t}$ and $\hat{\sigma_t}$ to be the estimate of θ and σ in the interval l. Considering the right censoring, the local log likelihood is obtained as

$$\begin{aligned} \log f(u_{t-l:t}|\theta_t) = & \sum_{i=2}^{n_t} w(t - u_i) \log f(u_i - u_{i-1}|H_{u_{i-1}}, \theta_t) \\ & + w(t - u_{n_t}) \log \int_{t-u_{n_t}}^{\infty} f(\vartheta|H_{u_{n_t}}, \theta_t)\, d\vartheta \end{aligned} \quad (9)$$

where $w(t)$ is the weighting function for the local likelihood estimation and we selected as $w(t) = e^{-\alpha(t-u)}$ with α as the weighting time constant that assigns the influence of a previous observation on the local likelihood at time t. As described previously [12], we employ an optimization procedure to estimate θ as well as σ. Since θ can be estimated in continuous time, at any time resolution, Δt, we can obtain the instantaneous estimate of all parameters and descriptors defined in Section II-A.

C. Model Goodness of Fit

The IBI probability model, along with the local maximum likelihood method, provides an approach for estimating the instantaneous parameters of the IBI distribution. These measures provide information about the changes in the characteristics of the distribution due to the irregularity of breathing. However, it is also essential to evaluate how well the model represents the IBI. To obtain a goodness-of-fit measure, we calculated the time-rescaled IBI defined as

$$\tau_k = \int_{u_{k-1}}^{u_k} \lambda\left(t|H_t, \hat{\theta}_t\right) dt \quad (10)$$

where u_k represents a point process observed in (0,T) and $\lambda(t|H_t, \hat{\theta}_t)$ is the conditional intensity function defined as

$$\lambda\left(t|H_t,\hat{\theta}_t\right) = f\left(t|H_t,\hat{\theta}_t,\hat{\sigma}_t\right) \times\left[1-\int_{u_{n_t}}^{t} f\left(\vartheta|H_\vartheta,\hat{\theta}_\vartheta,\hat{\sigma}_\vartheta\right)\,d\vartheta\right]^{-1}. \quad (11)$$

The conditional intensity is the history dependent rate function for a point process that generalizes the rate function for a Poisson process. The τ_k values are independent, exponential random variables with a unit rate. With a transformation $z_k = 1 - \exp(-\tau_k)$, if the model is correct, then z_k values are independent, uniform random variables on the interval (0,1]. Thus, we can employ a KS test to assess the agreement between z_k values and uniform probability density by computing a KS plot [8]. The KS distance measures the largest distance between the cumulative distribution function of the IBI transformed in the interval (0,1] and the cumulative distribution function of a uniform distribution on (0,1]. The smaller the KS distance, the better the model in terms of goodness of fit.

D. Experimental Data

To demonstrate our methodology, we considered IBI data from two different experiment protocols. The first set of IBI data was obtained from neonatal rats during spontaneous breathing. Neonatal rats exhibit respiratory patterns and chemoresponses analogous to preterm infants, including sporadic apneas with bradycardia and hypoxia, as well as periodically occurring apnea episodes. One to two day old rat pups were placed in a sealed chamber and breathed through a face mask and pneumotachogram, allowing recordings of respiratory airflow through the mask. The measurement of pressure within the plethysmographically sealed chamber was an index of respiratory effort. These previously published studies have documented the occurrence of irregular breathing patterns of central origin [13]. We analyzed 10 min of recordings during spontaneous breathing in each of four neonatal rats. The IBI time series was obtained by measuring the times of peak inspiratory airflow.

The preterm infant data considered in our analysis are associated with a wider study to understand control of breathing in preterm infants [7]. Data collection were conducted at the Newborn Intensive Care Unit, University of Massachusetts Memorial Hospital and approved by the Committee for the Protection of Human Subjects in Research at the University of Massachusetts Medical School. At the time of study, the infants' gestational age was less than 36 weeks and postconceptional age (PCA) was greater than 30 wks. These infants were breathing room air or supplemental oxygen through nasal cannulae at a fixed flow rate. Breathing was recorded using inductance plethysmography (Somnostar PT; Viasys Healthcare, Yorbalinda, CA, USA) at a sampling rate of 100 Hz. The IBI time series were derived from successive inspiratory peaks using a custom built peak detection program with a threshold of detection set at a level just above the small cardiac fluctuations. Nonrespiratory gross body movements are occasionally intermixed with respiratory signal during infant arousals. These signals were not excluded. We analyzed 10 min of recordings

from each of ten infants from one set of the study and considered 7 h of recordings from five infants from the second set.

III. Results

In this section, we first validate the performance of the model with the simulated dataset, and then we present the results from both the rat and infant datasets. The analysis includes the estimation of the parameters and the derivation of the descriptors, i.e., the indices of instability of breathing. The order p of the autoregressive model, $AR(p)$ is determined by the Akaike Information Criterion (AIC) [14] as primary point of reference, insuring at the same time an acceptable goodness-of-fit performance in terms of KS plots and autocorrelation functions. We studied the relationship of the derived descriptors with the physiology of infants and also evaluated further descriptors from the spectrum of the AR representation to capture the dynamics of breathing.

A. Analysis of Simulated IBI

To test the ability of our model to capture the correct probabilistic structure, we generated artificial IBI data from a log-normal distribution with a constant mean, $\mu = 0.1$ and constant $\sigma^2 = 0.16$. As an initial trial, we applied our model with the following parameters: a local likelihood window of length $W = 120$ *s*, time step $\Delta t = 0.15$ s, a weighting time constant $\alpha = 0.01$ and order $p = 8$ in the AR model.

Fig. 1 illustrates the estimated instantaneous mean and the instantaneous variance for one simulation. The KS plots of the time rescaled quantiles lies within the 95% confidence interval bounds and the autocorrelation function of the transform was indistinguishable from zero, both indicating the excellent goodness of fit. The averages of the estimated parameters are $\hat{\mu} = 0.108$ and $\hat{\sigma^2} = 0.158$, which are close to the actual values. These findings imply that our model can capture the stochastic lognormal behavior of IBI and can provide an accurate estimate of the mean as well as the variance.

Next we tested the ability of the model to track the changes in the variance σ^2, as such changes have been reported during a vibro-tactile stimulation provided to the infants using a mattress to reduce apnea episodes [7]. The ability of the model to track fast changes depends on the length of the likelihood window as well as the weighting time constant. To test such capability we simulated IBI values using the same parameters as previously described, and then we abruptly reduced the variance to 25% for a period of time (568 s), followed by restoration of the variance back to the original value. The adaptability of the model is illustrated in Fig. 2. In order to track abrupt changes, the model has to be less dependent on the history of IBI (i.e, rapidly forget the past) and have a fast weighting time constant. However, as we try to capture the abrupt transitions in variance, the model goodness of fit is affected as the model becomes sensitive to more subtle changes in IBI in a region where the variance should remain constant, thereby affecting goodness of fit. A trade-off strategy is therefore needed. Several simulated scenarios gave an empirical solution to the most appropriate combination choices for W, Δt, and α as a starting point before goodness-of-fit analysis.

B. Analysis of Neonatal Rat IBI

The experimental protocol employed to record respiratory signal from neonatal rats allows us to obtain IBI time series, free from any movement artifacts [13], which are very common in preterm infant recordings. Neonatal rat IBI data gives the opportunity to test our model in its ability of capturing the underlying probability distribution as well as the short-term dynamics of respiratory signals. This also allows us to test the model in terms of order and KS statistics prior to the application to the infant dataset.

Fig. 3 shows results from one of the recordings (R1). Here, the spectrogram in Fig. 3(b) represents the dynamic changes in IBI shown in Fig. 3(a) in the frequency domain. In this specific dataset, prior to apnea the two higher frequency oscillations merge and spread, suggesting that prior to impending apnea, the breathing signal shows the sign of instability. Similarly, the magnitude of the largest pole (predominant pole) of the system in Fig. 3(e) (black line) shows an increase in value prior to apnea.

Immediately after the apnea, the IBI dynamics retains the unstable pattern and gradually becomes stable. Fig. 3(c) and (d) potrays the μ and σ^2 estimated from the model, which also show significant changes prior to apnea. It has to be noted that the appearance of high frequency power and increase of pole magnitude observed prior to apnea is possibly due to the irregularity of breathing induced by the respiratory system.

Fig. 4 provides the goodness-of-fit measures using IBI data from all four rats. With the same parameter values for the model, the KS plots show different goodness-of-fit measures. In this case, although three of the data sets provide a better model fit to data, one rat (R4) did not provide a good fit to the model. However by reducing the history dependence we were able to fit the model well to data. Thus, neonatal rat data provides a way to study the effect of different parameters in capturing the information from artifact-free IBI data.

C. Analysis of Preterm Infant IBI

As first validation, we compared our lognormal-based model to a point process model with power law distribution. We defined the power law distribution as

$$f\left(t|\alpha_s\right)=\left[\frac{\alpha_s-1}{t_{min}}\right]\left(\frac{(t-u_k}{t_{min}}\right)^{-\alpha_s} \quad (12)$$

where$f\left(t|\ \alpha_s\right)$ is defined for $(t-u_k) > t_{\min}$, α_s is the exponent of the power law and $t_{\min}$ is the lower bound. We estimated the exponent α_s by maximizing the respective likelihood function as in (9) and compared goodness-of-fit results with the lognormal results. As expected, the lognormal-based model provides a better goodness of fit in all available data. Fig. 5 provides an exemplary analysis of the estimated α_s along with comparison of KS plots of the model with power law and lognormal distributions.

The preterm infant respiratory signal is highly nonstationary with rapid dynamic changes in physiological state. Our lognormal-based model could capture both fast dynamics as well as give an accurate representation of the stochastic structure underlying the IBI data recorded from the infants. Fig. 6 illustrates an example of IBI data along with the estimated μ and σ^2.

Here, it can be seen that σ^2 shows fast step increases both prior and during the apnea event. KS and autocorrelation plots suggest that the model is able to accurately capture the stochastic structure as well.

We also estimated the spectrum in the time frequency along with the dynamics of the predominant pole. The example in Fig 7 (same subject as in Fig 6) shows how both spectrum and predominant pole can provide the additional dynamic measures of IBI instability that may be a precursor of apnea.

Since apnea, a pause in breathing, is common in preterm infants, we studied the effect of such a pause on the instability of breathing. From the database, we considered infants with at least 7 h of physiological recordings. We identified only those apnea events that are 10 s or greater and did not have any such apneas 10 min prior to this event. Fig. 8 demonstrates the instability of breathing in terms of IBI observed in the time-frequency plane. The integrated power spectrum dynamics is significantly larger after the apnea episodes, which indicates that the apnea episode introduces instability in the IBI and instability is maintained for a long time, in this case, at least three minutes after the apnea episodes.

We also estimated the poles of the autoregressive process as a measure of instability of breathing from an infant during an episode of apnea. The distribution of the predominant pole after 10 min of the apnea episode is different from prior 10 min of the episode. Fig. 9 represents the dynamics of predominant pole along with the histogram of the pole magnitude prior 10 min and the post 10 min of the apnea episode.

D. Statistical Analysis

We studied the relationship of all the derived descriptors (appropriately averaged for each subject and then for all subjects) to the physiological variables of ten preterm infants. Table I reports the linear Pearson correlation along with the *P*-value in brackets for the preterm infants. It should be noted that *S* and *K* correlate with the PCA and weight of the infant at the time of study (SW), which suggest that these two descriptors provide information about the maturation of the infants. As the infant matures, the probability of apnea reduces, which will reflect in more skewness and kurtosis of the distribution.

The variance *V* correlates with all physiological variables including gestational age (GA) and weight of the infant at the time of birth (BW). We also computed Spearman's correlation coefficient to look for any nonparametric dependence between indices and physiological variables. We found that variance *V* still correlates with GA, BW, and SW with linear correlations (*P*-Value) 0.78 (0.03), 0.85 (0.01) and 0.84(0.01), respectively. However, *V* did not correlate with PCA and also none of the other indices had any significant correlations with physiological variables, except for *M* and GA with 0.73 (0.04).

We studied the variability of the indices in the subjects by considering every 10 s or greater apnea episodes in all the five subjects. There were a total of 27 apnea episodes from five subjects: 7 from s1, 4 from s2, 3 from s3, 10 from s4, and 3 from s5. We found that the variance of the respiratory rate (see table II) is significantly greater after the apnea episode when compared to values before the episode. This is important considering the fact that,

after the apnea, the infant's effort to breathe increases introducing a significant variability in the respiratory rate. All other measures increase after apnea, although not significantly, except M and M_r.

To understand which of the descriptors carries more information on the transition before and after the apnea event, we finally performed a simple discriminant analysis by moving a linear separating threshold to obtain the receiver operating characteristics (ROC) curve for each descriptor and for each combination of two descriptors. Results are reported in table III and the ROC curves from the most discriminating descriptors are shown in Fig. 10. We found that the best discrimination between before and after apnea is obtained from *S*, *K*, and the *Pole Magnitude* if considering a single descriptor. Combining *S* and *Pole Magnitude*, we obtain the absolute best discrimination (37% specificity and 67% sensitivity), followed by the *M-Pole Magnitude* combination (37% specificity and 63% sensitivity), and the *K-Pole Magnitude* combination (37% specificity and 63% sensitivity).

IV. Discussion

We have developed a point process modeling framework and algorithm for analyzing the instability of breathing in neonates. Our point process modeling framework provides instantaneous descriptors of instability that can be defined as important precursors of apnea events in individual infants.

Our algorithm is based on the observation that the IBI poses stochastic characteristics with a long tail distribution and dynamic characteristics with apneas related to low frequency oscillations in breathing. We employed a lognormal distribution on a point process modeling framework to capture the stochastic characteristics, and a higher order autoregressive model to capture the instability of IBI associated with apnea and other irregularities in the breathing patterns of infants.

The advantage of using a point process framework is that the probability density can be computed at any time resolution regardless of the duration of IBI. Furthermore, the estimation of instantaneous indices as well as the power spectrum provides measures to assess the physiologic development of infants in real time. The goodness-of-fit tests allow us to select the appropriate order as well as history dependence and to assess the ability of the model to capture the data.

In the future, we plan to implement our model in the newborn intensive care unit to assess the instability of breathing as well as maturation of neonates. We will also study whether using other representations can capture the dynamic characteristics of the IBI as well, such as Volterra series representations [15], [16], and perturbation series representation of oscillator models [17] related to respiration.

In our analysis, we assumed that the IBI series follows a distribution with lognormal characteristics. Since it has been hypothesized that different stochastic properties may appear during periodic breathing [5], one of our future goals is to verify if the IBI series may be switching between two different types of distribution, in particular between a lognormal distribution and a separate distribution associated with periodic breathing. To this extent, the

probabilistic representation must include different types of distributions. We plan to explore such possibilities in the IBI dynamics and if we observe such a phenomenon, then we will modify the algorithms to include a multimodal distribution framework [18]. We will estimate the parameters based on the optimization of the likelihood function of this multimodal structure.

In addition, by integrating the point process model of IBI along with the point process model of heart-rate dynamics [12], [19], we will study whether these models can be used for the anticipation of life threatening events such as apnea, bradycardia, and hypoxia in neonates. Recent work in mice reveals critical periods in the vulnerability of cardio-respiratory control to genetic perturbations, for example in 5-HT_{1A} knockout mice that exhibit subtle abnormalities in breathing and heart-rate variability [20]. We propose that the point process framework can define novel dynamical biomarkers that reflect intrinsic vulnerabilities of cardio-respiratory control.

We used respiratory inductive plethysmography to define breathing patterns in preterm infants as previously described [7]. This method detects apnea due to a failure of centrally generated inspiratory effort, which is the most common mechanisms of apnea initiation in preterm infants during sleep [21]. Our results, therefore, pertain to central apnea. Obstructed breaths occasionally appear during periods of prolonged central apnea, manifesting as abdominal movements that are indistinguishable from an unobstructed breaths using inductance plethysmography alone. The proof of obstructive apnea would require simultaneous measurement of respiratory airflow, which is difficult to obtain in infants. Future studies that include airflow signals would be needed to determine how obstructed breaths influence the statistical properties of the IBI time series and howto capture this in the point process framework.

It is also important to note that our infant respiratory recordings, while highly sensitive for detecting central apnea during quiet sleep, cannot reliably distinguish respiratory movement from other types of axial movements that might occur during brief arousals. Since transient arousal can be a strong destabilizing influence on breathing [21], future studies are needed to test the hypothesis that movement *per se* is a precursor of apnea. This movement information is already being captured in our point process model of IBI, as the movement signal is intermixed with the respiratory signal during arousal.

In conclusion, given the promising discrimination results and the prospect of being able to consider larger datasets and of applying more advanced classification techniques, we are confident that the proposed descriptors could provide an accurate assessment, monitoring, and prediction of the risk of infants to impending apnea events.

Acknowledgments

The authors would like to thank E. Salisbury, F. Bednarek, E. N Brown, C. Dunn, and I. Zuzarte for discussions during the course of this study. They would also like to thank K. Cummings for providing data from his experiments on newborn rats [13] and R. Sclocco for the help in linear discriminant analysis.

This work was supported in part by the Hansjörg Wyss Institute for Biologically Inspired Engineering at Harvard University and in part by the National Institutes of Health under Grant R01-HL084502, Grant R01-HL49848, Grant R01-HL071884, Grant R01-GM104987

References

1. Feldman JL, Del Negro CA. Looking for inspiration: New perspectives on respiratory rhythm. Nat Rev Neurosci. Mar; 2006 7(3):232–242. [PubMed: 16495944]
2. Abu-Shaweesh JM, Martin RJ. Neonatal apnea: What's new? Pediatr Pulmonol. Oct; 2008 43(10): 937–944. [PubMed: 18780339]
3. Poets CF. Interventions for apnea of prematurity: A personal view. Acta Paediatr. Feb; 2010 99(2): 172–177. [PubMed: 19958303]
4. Frey U, Silverman M, Barabasi AL, Suki B. Irregularities and power law distributions in the breathing pattern in preterm and term infants. J Appl Physiol. Sep; 1998 85(3):789–97. [PubMed: 9729549]
5. Waggener TB, Frantz ID III, Stark AR, Kronauer RE. Oscillatory breathing patterns leading to apneic spells in infants. J Appl Physiol. May; 1982 52(5):1288–1295. [PubMed: 7096153]
6. Picone S, Bedetta M, Paolillo P. Caffeine citrate: When and for how long. A literature review. J Matern Fetal Neonatal Med. Oct.2012 25:11–4. [PubMed: 23016611]
7. Bloch-Salisbury E, Indic P, Bednarek F, Paydarfar D. Stabilizing immature breathing patterns of preterm infants using stochastic mechanosensory stimulation. J Appl Physiol. Oct; 2009 107(4): 1017–1027. [PubMed: 19608934]
8. Brown EN, Barbieri R, Ventura V, et al. The time-rescaling theorem and its application to neural spike train data analysis. Neural Comput. Feb; 2002 14(2):325–346. [PubMed: 11802915]
9. Indic P, Paydarfar D, Barbieri R. A point process model of respiratory dynamics in early physiological development. Proc IEEE Eng Med Biol Soc Conf. 2011; 2011:3804–7.
10. Mitzenmacher M. A brief history of generative models for power law and lognormal distributions. Internet Math. 2003; 1(2):226–251.
11. Navarro X, Poree F, Beuchee A, Carrault G. Respiration signal as a promising diagnostic tool for late onset sepsis in premature newborns. Comput Cardiol. 2010; 37:947–950.
12. Barbieri R, Matten EC, Alabi AA, Brown EN. A point-process model of human heartbeat intervals: new definitions of heart rate and heart rate variability. Amer J Physiol Heart Circ Physiol. Jan; 2005 288(1):H424–35. [PubMed: 15374824]
13. Cummings KJ, Frappell PB. Breath-to-breath hypercapnic response in neonatal rats: temperature dependency of the chemoreflexes and potential implications for breathing stability. Amer J Physiol Regul Integr Comput Physiol. Jul; 2009 297(1):R124–134.
14. Priestley, MB. Spectral Analysis and Time Series. New York, NY, USA: Academic; 1983.
15. Chen Z, Brown EN, Barbieri R. Characterizing nonlinear heartbeat dynamics within a point process framework. IEEE Trans Biomed Eng. Jun; 2010 57(6):1335–1347. [PubMed: 20172783]
16. Chon KH, Mukkamala R, Toska K, Mullen TJ, Armoundas AA, Cohen RJ. Linear and nonlinear system identification of autonomic heart-rate modulation. IEEE Eng Med Biol Mag. Sep-Oct;1997 16(5):96–105. [PubMed: 9313086]
17. Indic P, Brown EN. Characterizing the amplitude dynamics of the human core-temperature circadian rhythm using a stochastic-dynamic model. J Theor Biol. Apr; 2006 239(4):499–506. [PubMed: 16223510]
18. Chen Z, Vijayan S, Barbieri R, Wilson MA, Brown EN. Discrete- and continuous-time probabilistic models and algorithms for inferring neuronal up and down states. Neural Comput. Jul; 2009 21(7):1797–1862. [PubMed: 19323637]
19. Barbieri R, Brown EN. Analysis of heartbeat dynamics by point process adaptive filtering. IEEE Trans Biomed Eng. Jan; 2006 53(1):4–12. [PubMed: 16402597]
20. Barrett KT, Kinney HC, Li AH, Daubenspeck JA, Leiter JC, Nattie EE. Subtle alterations in breathing and heart rate control in the 5-HT1 A receptor knockout mouse in early postnatal development. J Appl Physiol. Nov; 2012 113(10):1585–1593. [PubMed: 22936722]
21. Paydarfar, D.; Buerkel, M. Collapse of homeostasis during sleep. In: Schwartz, WJ., editor. Sleep Science: Integrating Basic Research and Clinical Practice. Basel, Switzerland: Krager; 1997. p. 60-85.

Biographies

Premananda Indic (M'10) received the B.Tech. degree in electrical and electronics engineering, the M.Tech. degree in electrical engineering from the University of Calicut, Kozhikode, Kerala India, the Ph.D. degree from the Cochin University of Science and Technology, Thrikkakara, Kerala, India.

He did the Post Doctoral training from Harvard Medical School, Boston, MA, USA. He is currently a Research Assistant Professor in the Department of Neurology, University of Massachusetts Medical School, Worcester, USA. The major goal of his research is to develop signal processing algorithms to detect as well as anticipate the abnormal behaviors of the physiological signals and develop appropriate countermeasures to control the dynamics of the physiological systems. His research interests include understanding apnea, epilepsy, and circadian dysrhythmias from the corresponding physiological signals.

David Paydarfar received the B.S. degree in physics from Duke University, Durham, NC, USA, the M.D. degree from the University of North Carolina at Chapel Hill, Chapel Hill, NC, and Postgraduate training in neurology at the Massachusetts General Hospital, Boston, MA, and Harvard Medical School.

He is currently a Professor and Vicechair of neurology at the University of Massachusetts Medical School, and the Associate Faculty at the Wyss Institute for Biologically Inspired Engineering at Harvard University. His research interests include to develop new approaches for quantifying and controlling oscillatory behavior at the cellular, tissue and organism levels, and applying these insights to treat pathological conditions, for example preventing apnea of prematurity related to pathological pauses in the central respiratory oscillator.

Dr. Paydarfar is a Fellow of the American Neurological Association.

Riccardo Barbieri (M'00–SM'08) was born in Rome, Italy, in 1967. He received the M.S. degree in electrical engineering from the University of Rome "La Sapienza", Rome, Italy, in 1992, and the Ph.D. degree in biomedical engineering from Boston University, Boston, MA, USA, in 1998.

He is an Assistant Professor of anaesthesia at Harvard Medical School—Massachusetts General Hospital and Research Affiliate at the Massachusetts Institute of Technology, Cambridge, USA. He is currently focusing his studies on computational modeling of neural information encoding, and on application of nonlinear and multivariate statistical models to characterize heart rate variability and cardiovascular control dynamics. He is author of more than 70 peer-reviewed publications in these fields since 1994. His research interests include the development of signal processing algorithms for the analysis of biological systems.

Dr. Barbieri is a member of the American Association for the Advancement of Science, the European Society of Hypertension, the Society for Neuroscience, and the Engineering in Medicine and Biology Society.

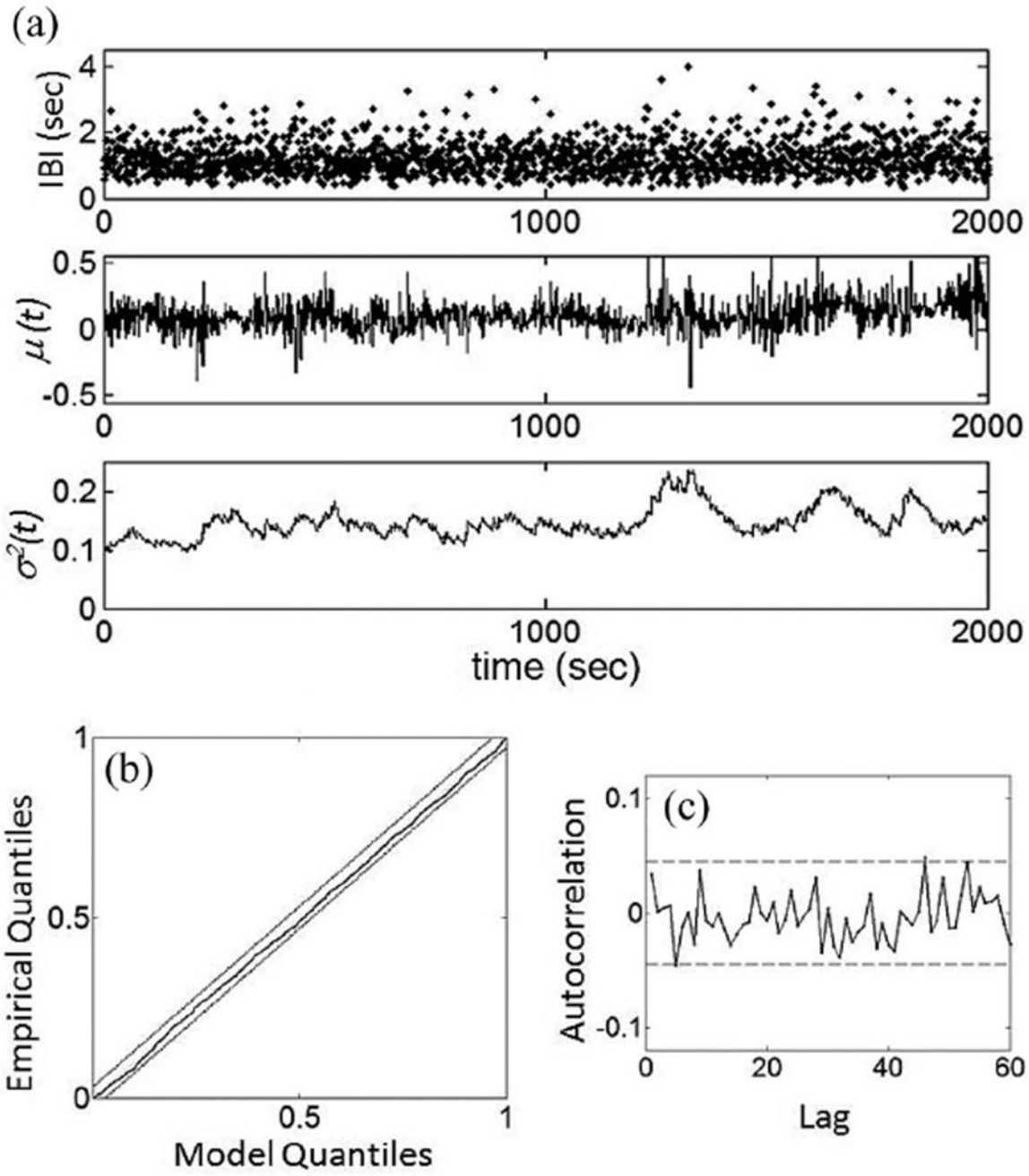

Fig. 1.

(a) Instantaneous time varying estimates μ and σ for the simulated IBI with local likelihood window $W = 120$ s, time step $\Delta t = 0.15$, $\alpha = 0.01$, and $p = 8$ (b) KS plot (black line) of the time-rescaled quantiles derived from the model. (c) Autocorrelation function of the transformed times estimated for the first 60 lags. The dotted lines represent the 95% confidence intervals.

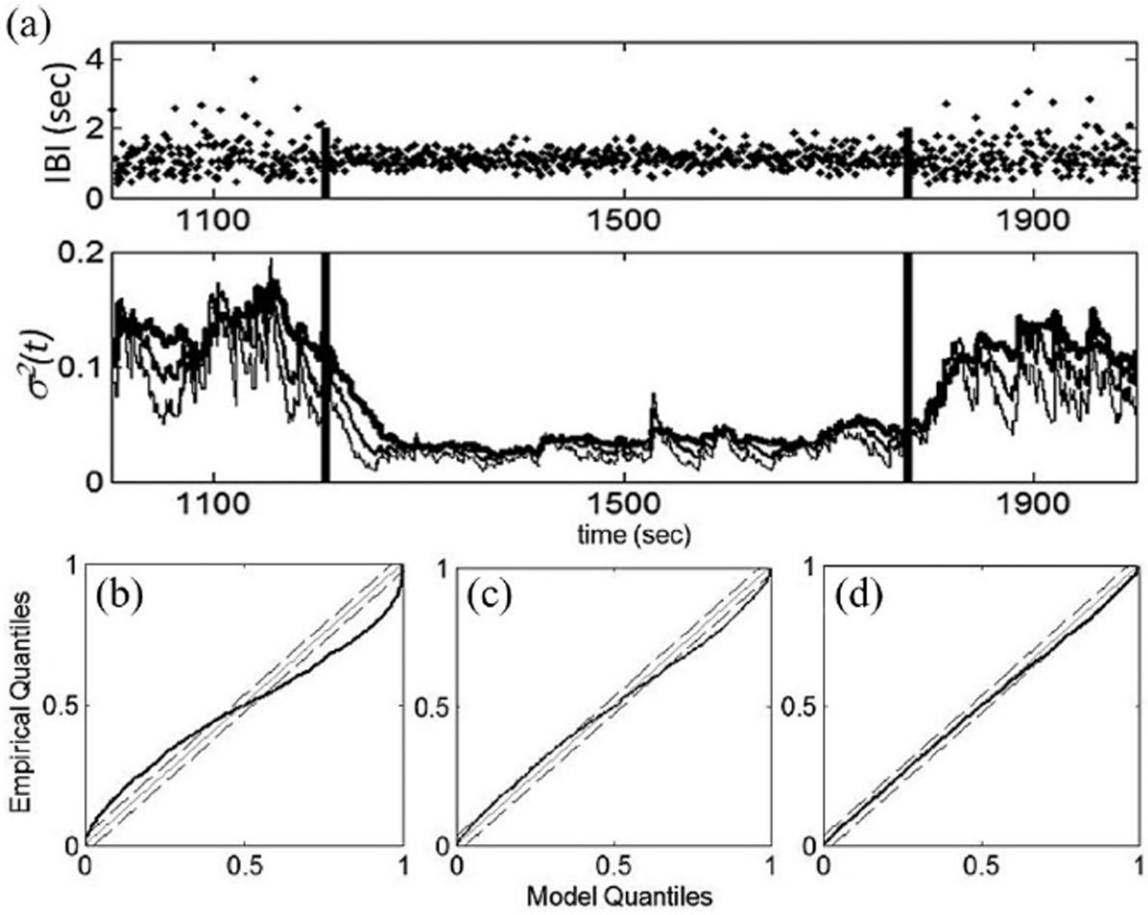

Fig. 2.

(a) Simulated IBI with transitions in variance marked by vertical solid bars along with instantaneous estimate of σ^2 for the simulated IBI with $p = 8$, $W = 120$ s at a time resolution $\Delta t = 0.15$ Thin line represents $\alpha = 0.1$, medium line represents $\alpha = 0.05$, and the bold line represents $\alpha = 0.01$. The corresponding KS plots are shown in (b), (c), and (d), respectively.

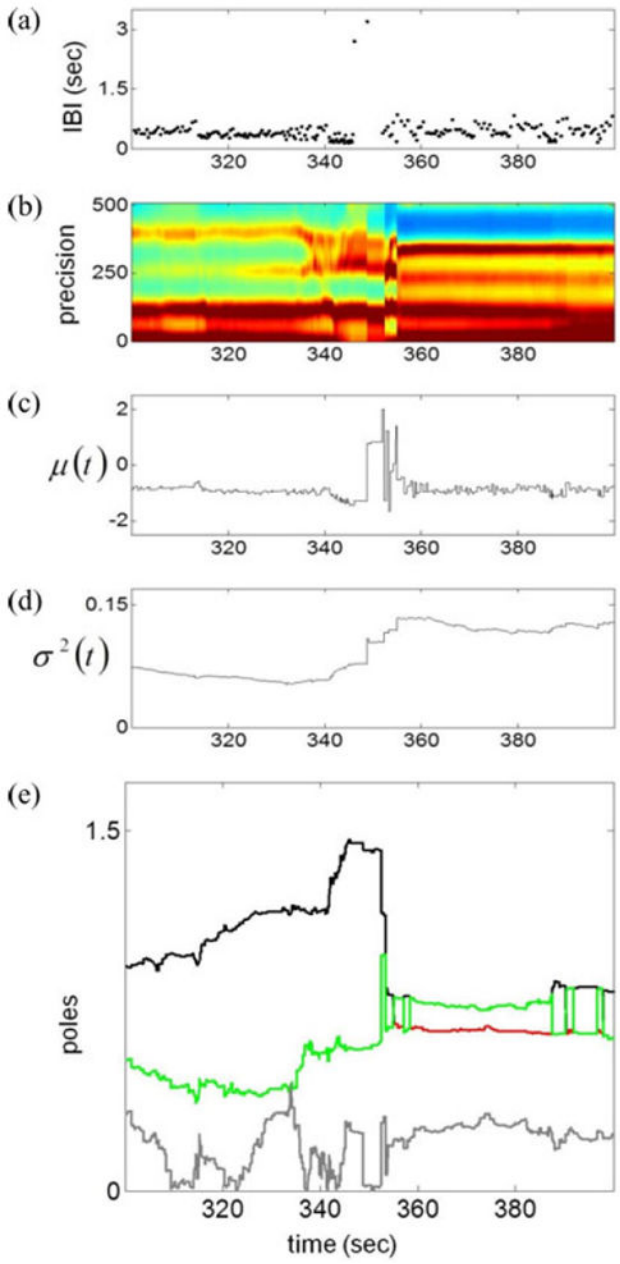

Fig. 3.

Point process estimate of instantaneous measures of a representative rat data. (a) IBI values derived from the neonatal rata breathing patterns. The normal IBI is ~0.4 and ~3 s IBI is considered as a severe apnea. (b) Power spectrum representation on a 512 precision scale. The instantaneous estimate of (c) μ and (d) σ^2. (e) Dynamics of poles obtained from AR(4) model.

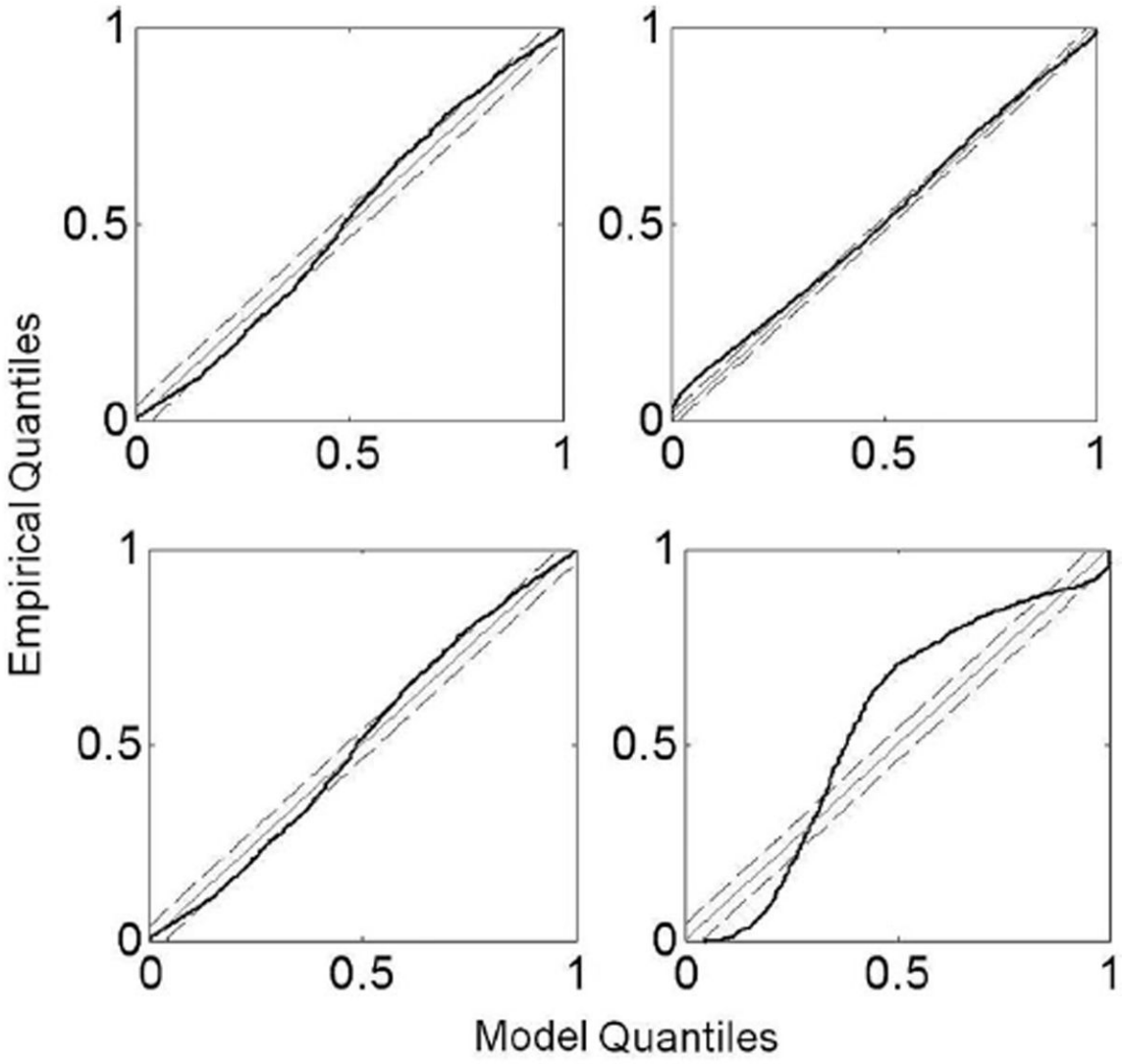

Fig. 4.

KS plots of the time-rescaled quantiles derived from the spontaneous breathing of four neonatal rats (R1–R4).

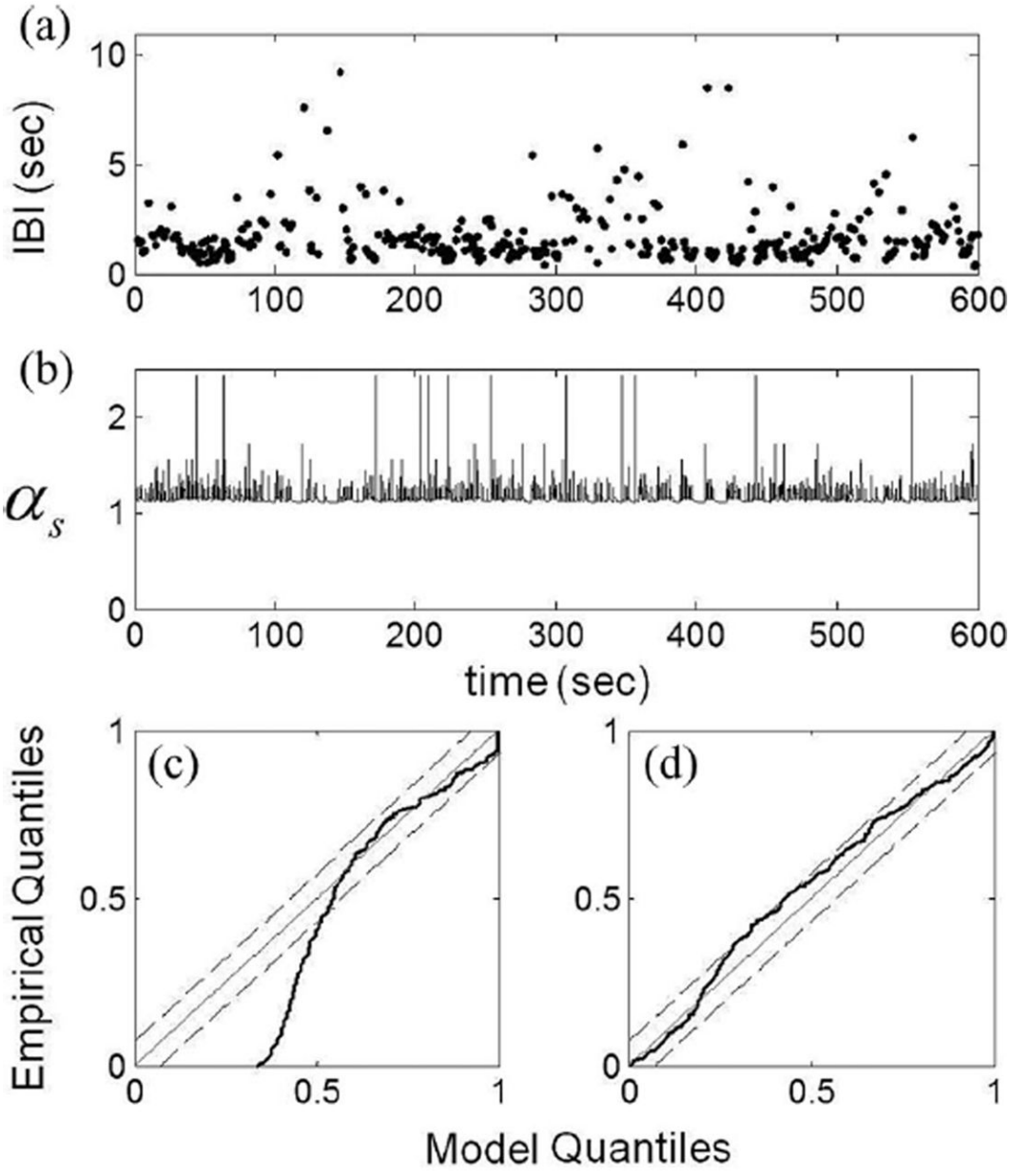

Fig. 5.

Point process estimate of IBI data using a power law distribution. (a) IBI from an infant and (b) instantaneous estimation of power law exponent α_s. The average value of the exponent is obtained as 1.16. (c) KS plot of the time rescaled quantiles and (d) corresponding KS plot of the point process model with lognormal distribution.

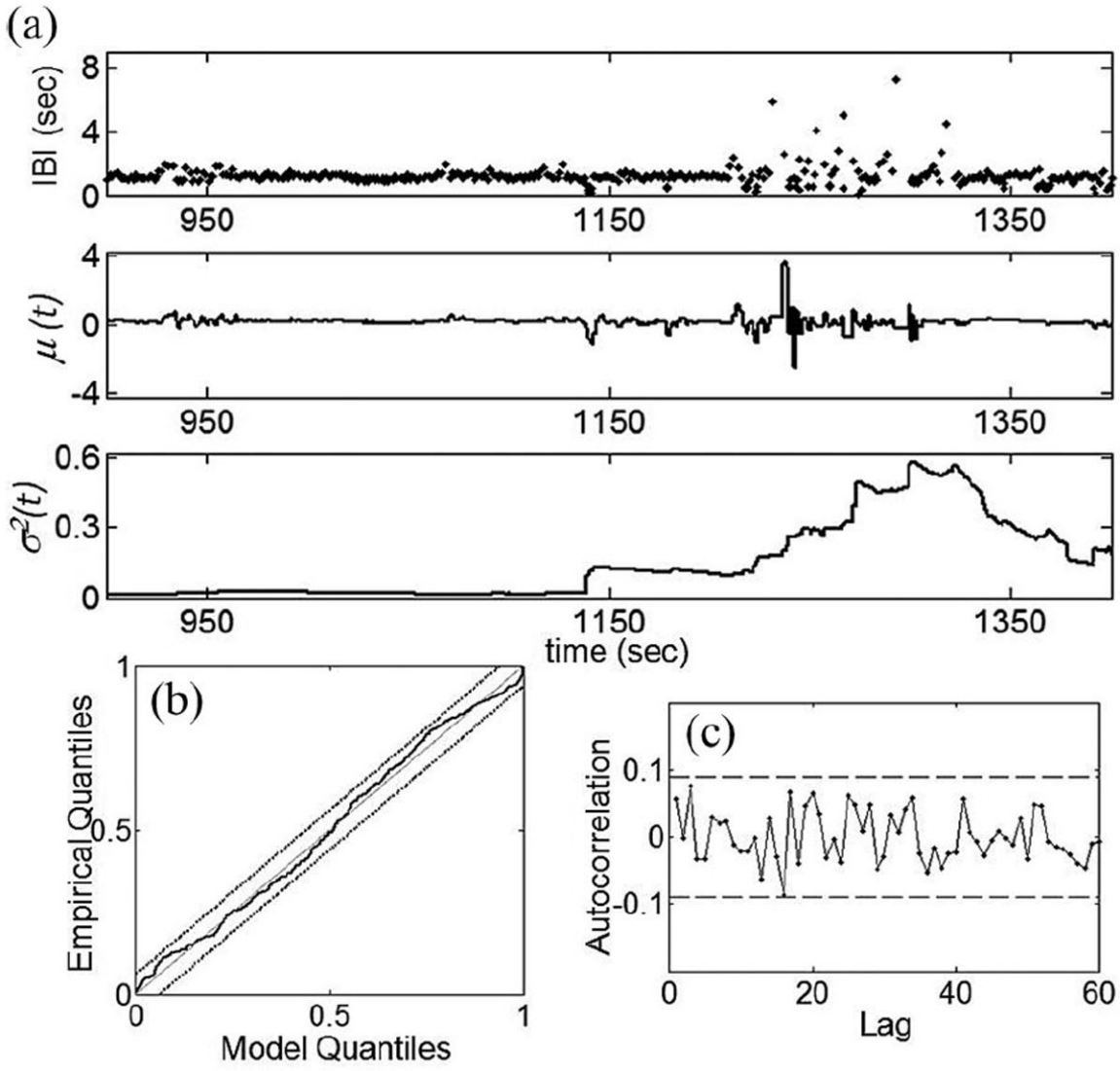

Fig. 6.

(a) Instantaneous time varying estimates μ and σ^2 for the IBI data from a preterm infant with local likelihood window W = 120 s, time step Δt = 0.05, α = 0.01 (optimized by KS analysis), and p = 4 (optimized by AIC, autocorrelation function, and KS analysis). (b) KS plot (black line) of the time-rescaled quantiles derived from the model. (c) Autocorrelation function of the transformed times estimated for the first 60 lags. The dotted lines represent the 95% confidence intervals.

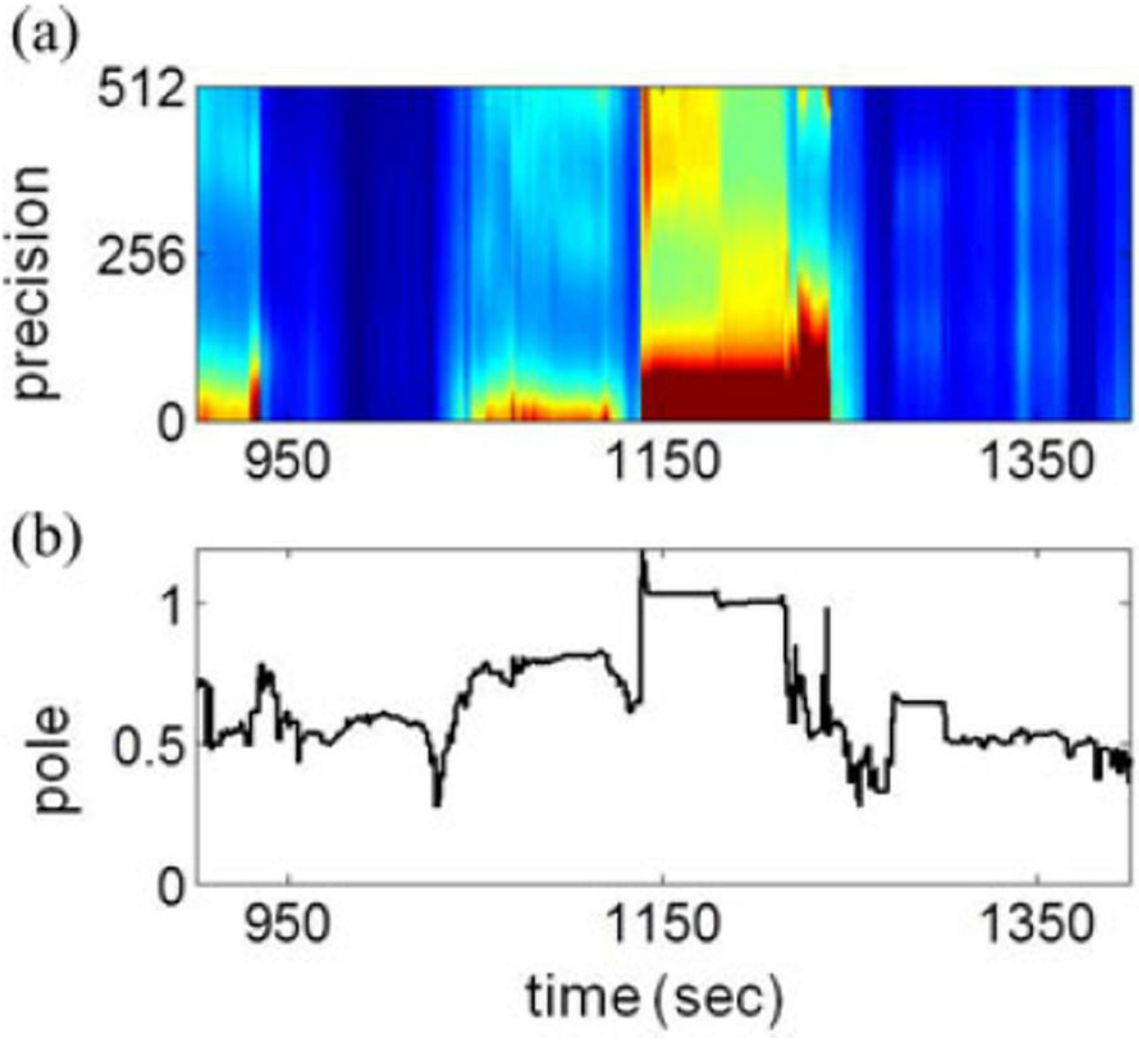

Fig. 7.

(a) Instantaneous time varying estimates of spectrum on a 512 precision. (b) Dynamics of predominant pole for the same IBI data represented in Fig 6(a).

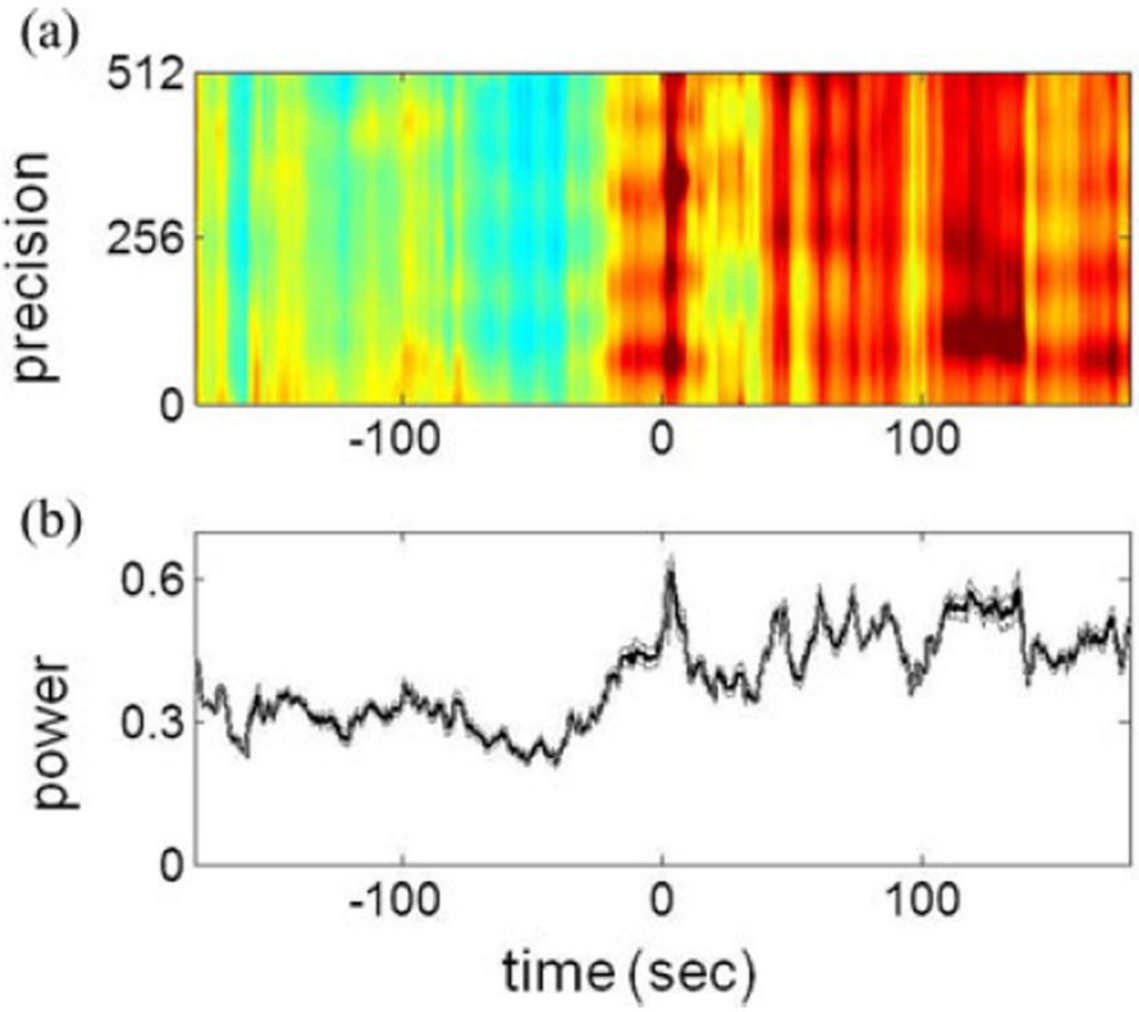

Fig. 8.

(a) Average power spectrum in a time frequency representation for the IBI data from a preterm infant with ten apnea episodes. Zero on time axis represents the time of apnea event. (b) Average integrated power (black line) along with the 95% confidence interval (gray line). The average power is significantly different prior and post apnea events with a P-value < 0.001.

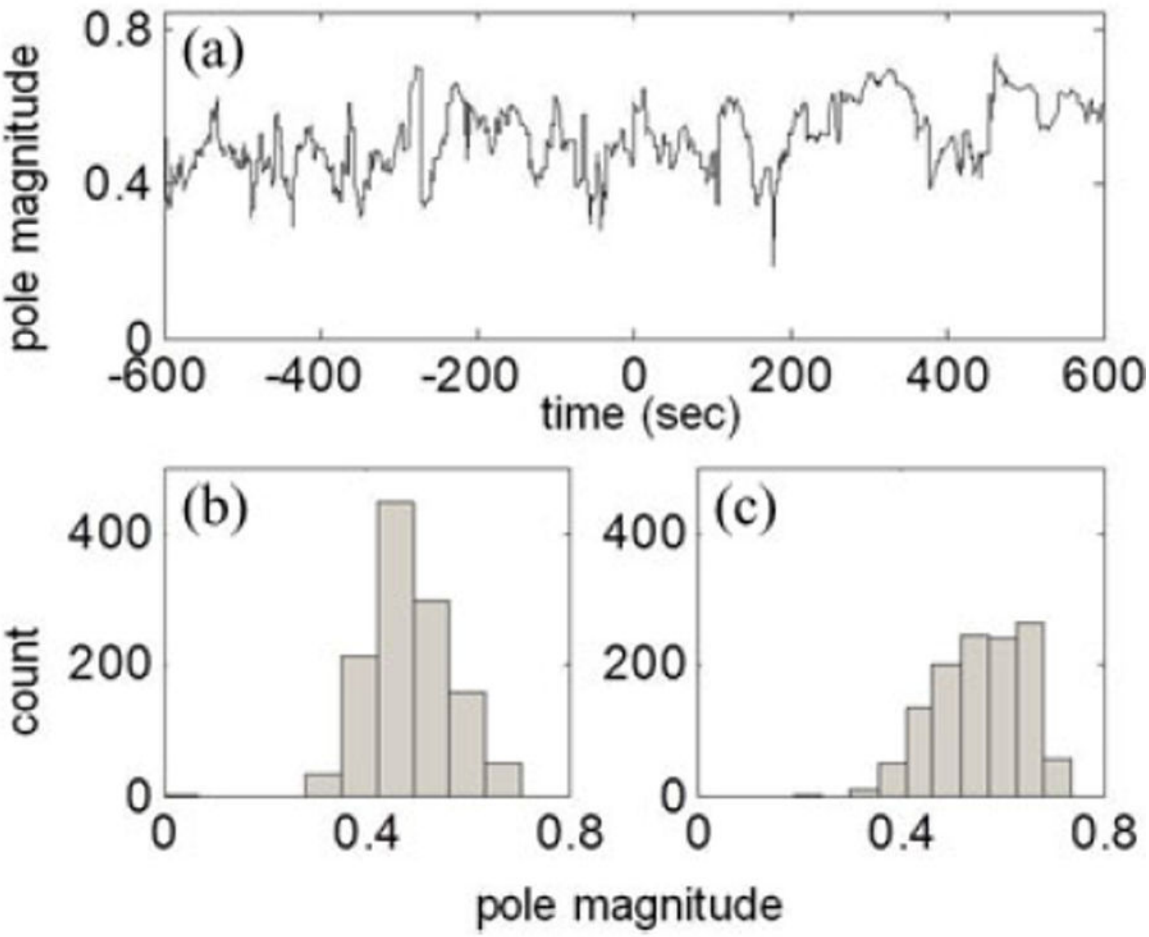

Fig. 9.

Magnitude of the predominant pole estimated using an AR(4) autoregressive model from an infant (a) dynamics of the predominant pole, (b) histogram of pole magnitude 10 min prior to the apnea episode. (c) Histogram of pole magnitude 10 min after the apnea episode. Values are divided into 10 bins.

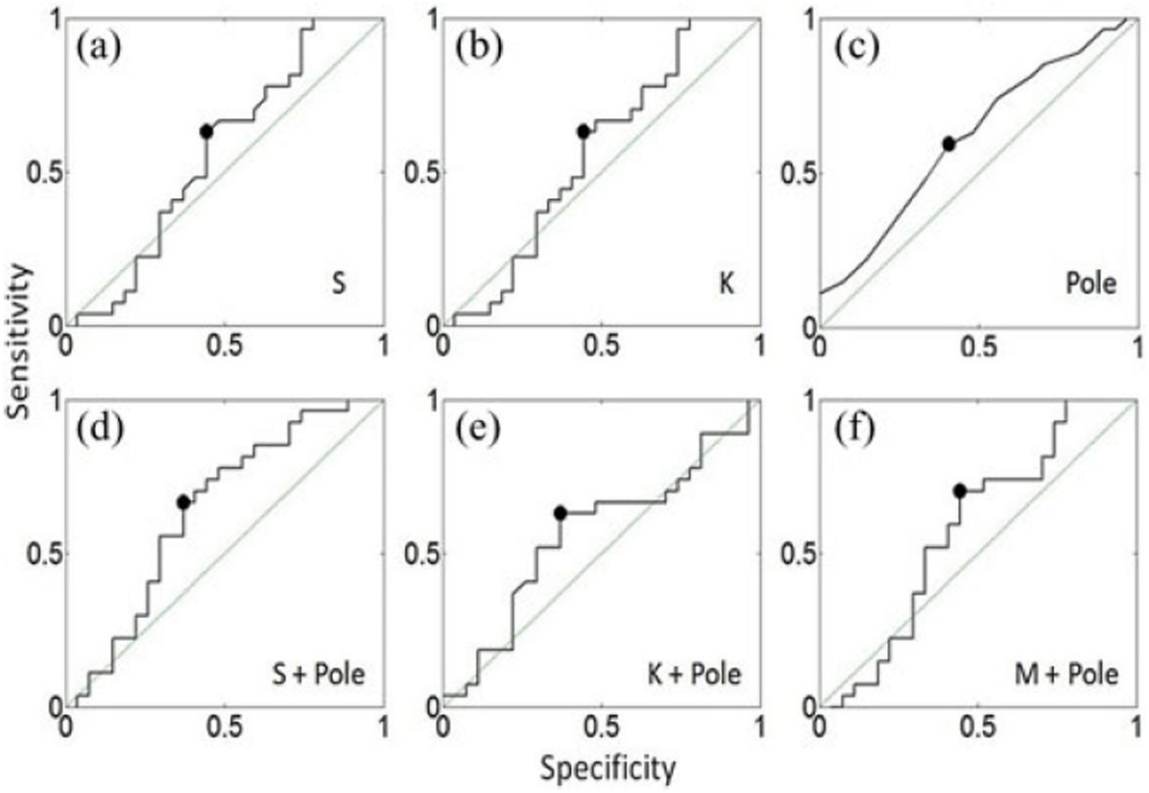

Fig. 10.

Best ROC curves obtained from the discriminant analysis for measures (a) S, (b) K, and (c) Pole Magnitude, as well as for (d) the selected combinations S and Pole Magnitude, (e) K and Pole Magnitude, and (f) M and Pole Magnitude. Black dots indicate the points at minimum distance from the upper left corner. Specificity, sensitivity, and distance at these points are reported in table III.

TABLE I

Linear Correlations (*P*-Value) Between the Indices Obtained from the Model and the Physiological Variables

Descriptors	Physiological Variables			
	GA	PCA	BW	SW
M	0.51 (0.20)	0.30 (0.47)	0.56 (0.15)	0.39 (0.35)
V	0.73* (0.04)	0.80* (0.02)	0.76* (0.03)	0.89* (0.01)
S	0.61 (0.11)	0.72* (0.04)	0.63 (0.09)	0.79* (0.02)
K	0.62 (0.10)	0.73* (0.04)	0.62 (0.10)	0.79* (0.02)
$\mathbf{M_r}$	0.33 (0.43)	0.48 (0.23)	0.32 (0.44)	0.51 (0.19)
$\mathbf{V_r}$	0.56 (0.15)	0.69 (0.06)	0.55 (0.16)	0.74* (0.04)

* Represents significant correlations with a *P*-value less than 0.05.

TABLE II

Mean (SD) of Instantaneous Measures of all Apnea Episodes From Five Infants

MEASURES	Before	After
M	2.07 (0.73)	2.04 (0.73)
V	0.85 (0.52)	0.89 (0.47)
S	5.85 (0.47)	6.06 (0.78)
K	3.77 (1.51)	4.54 (2.60)
$\mathbf{M_r}$	0.92 (0.03)	0.91 (0.04)
$\mathbf{V_r}$	0.09* (0.05)	0.12* (0.10)
Spectrum	0.47 (0.31)	0.54 (0.47)
Pole Magnitude	0.52 (0.03)	0.53 (0.04)

* Represents significant correlations with a *P*-value less than 0.05.

TABLE III

Sensitivity and Specificity of Measures in Discriminating Dynamics 10 Min Before and 10 Min After the Apnea

MEASURES	SPECIFICITY	SENSITIVITY	DISTANCE
M	0.48	0.56	0.43
V	0.41	0.55	0.36
S	0.44	0.63	0.33
K	0.44	0.63	0.33
$-M_r$	0.44	0.55	0.39
V_r	0.37	0.52	0.46
Spectrum	0.48	0.52	0.46
Pole Magnitude	0.41	0.59	0.33
Best Combination by Considering Two Measures			
S+Pole Magnitude	0.37	0.67	0.25
M+Pole Magnitude	0.37	0.63	0.27
K+Pole Magnitude	0.44	0.70	0.28
V_r+Pole Magnitude	0.33	0.52	0.34
S+K	0.44	0.63	0.33
V+V_r	0.48	0.67	0.34
S+V_r	0.30	0.48	0.36
V+Pole Magnitude	0.22	0.44	0.36
V+S	0.41	0.55	0.35
V+M	0.30	0.48	0.36